Asian Journal of Chemistry; Vol. 36, No. 10 (2024), 2269-2274

ASIAN JOURNAL OF CHEMISTRY

https://doi.org/10.14233/ajchem.2024.32215

Synthesis and Characterization of Ester Derivatives of N-Phenylanthranilic Acid

MADHU BALA[1,2,*], RACHNA YADAV[1] and AMIT GIRDHAR[1]

[1]Department of Chemistry, Shri Khushal Das University, Hanumangarh-335801, India
[2]Department of Chemistry, JCD Memorial College, Jan Nayak Ch. Devi Lal Vidyapeeth, Sirsa-125056, India

*Corresponding author: E-mail: madhukakkar14@gmail.com

Received: 11 June 2024; *Accepted*: 24 July 2024; *Published online*: 30 September 2024; AJC-21756

N-Phenylanthranilic acid (fenamic acid) serves as the fundamental structure for synthesizing several non-steroidal anti-inflammatory drugs, antibacterial drugs and also functions as a modulator of membrane transport. To reduce the dose-related side effects of existing drugs, research is focussing to improve fenamic acid derivative solubility and bioavailability. A series of ester derivatives of N-phenylanthranilic acid (**MB-1** to **MB-5**) *viz*. 2-(phenyl amino)methyl benzoate, 2-(phenyl amino)ethyl benzoate, 2-(phenyl amino)isopropyl benzoate, 2-(phenyl amino)butyl benzoate and 2-(phenyl amino)phenyl benzoate were synthesized. The chemical structures and functional groups of these derivatives were confirmed using elemental analysis and spectral data. Furthermore, the derived compounds were evaluated for their antibacterial activity against *Escherichia coli* (Gram-negative) and *Staphylococcus aureus* (Gram-positive) strains using the agar-well diffusion method followed by molecular docking studies to predict binding interactions of the synthesized compounds with DNA gyrase.

Keywords: N-Phenyl anthranilic acid, Ester derivatives, Antimicrobial activity, Antibacterial activity, Agar-well diffusion.

INTRODUCTION

For the synthesis of benzo-fused heterocycles, anthranilic acid, chemically known as 2-aminobenzoic acid, is a flexible and affordable base material [1]. While developing drugs to manage the pathophysiology and etiology of different diseases, N-phenyl anthranilic acid and its derivatives provide a unique profile as pharmacophores and basic skeleton molecules [2]. The synthesis of several commercially available drugs including furosemide (diuretic), tranilast (anti-allergic), betrixaban (anticoagulant) and fenamates (analgesic and anti-inflammatory agents), is thought to be facilitated by these derivatives (Fig. 1), which are also thought to be an inexpensive and effective starting precursor. In last 30 years, a number of anthranilic acid analogs have shown diverse biological activities, including insecticidal, antiviral, anticancer, antibacterial and anti-inflammatory properties [3].

In past, N-phenyl anthranilic acid was used in research to cause and observe renal papillary necrosis in rats [4] and the pharmacological characteristics of derivatives of fenamic acid as a novel anti-atopic drug were determined [5]. From these studies, these precursors and compounds exhibited influential antiviral, anticancer and antidiabetic activities. The functional head groups of anthranilic acid and its analogues, such as carboxyl, amino, amide, carbomethoxy and acetamide, enable their conjugation and derivatization to produce well-designed molecules meant to interact with their biological targets [6-8].

N-Phenyl anthranilic acid (fenamic acid), a derivative of anthranilic acid and a nitrogen isostere of salicylic acid, functions as active metabolite of aspirin, paving the way for more refined research in medicinal chemistry [9]. Fenamates are clinically employed as non-steroidal anti-inflammatory drugs (NSAIDs) for the treatment of fever, pain and inflammation [10]. These small compounds work by preventing the cyclooxygenase (COX) enzyme from acting, which lowers prostaglandin biosynthesis [11,12]. Additionally, fenamates have low-potency modulatory effects on a variety of enzymes and ion channels, acting as either activators or inhibitors. Fenamates, for instance, activate large-conductance Ca^{2+} activated K^+ (Slo1) channels [13-15], transient receptor potential ankyrin-1 channels (Hu) and Ca^{2+} activated Cl^- channels [16,17], ATP-sensitive K^+ channels [18] and non-selective cation channels [19]. As NSAIDs,

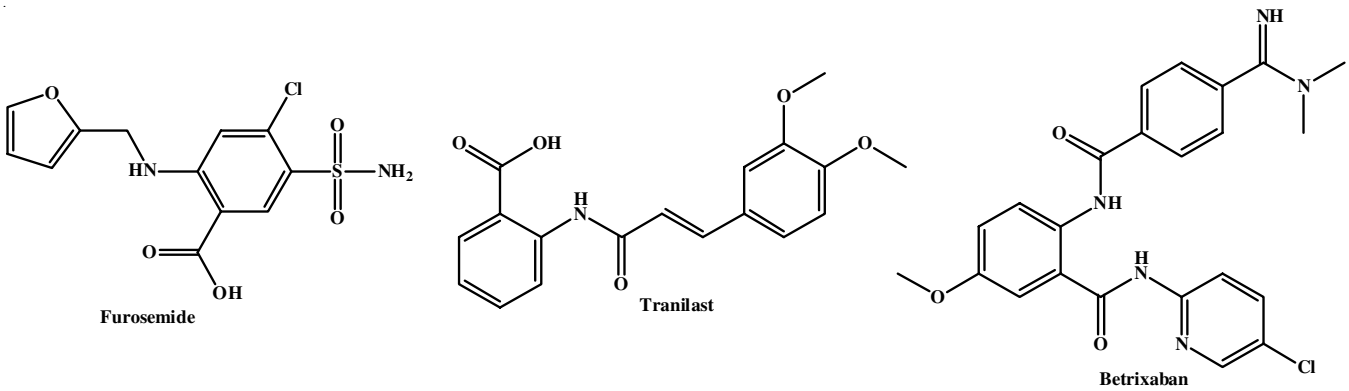

Fig. 1. Chemical structures of furosemide, tranilast and betrixaban

fenamates represent an intriguing class of drugs that may be exploited to combine other targets with strong GABAa receptor allosteric agonists to reduce pain, inflammation and the corresponding anxiety and depression. Headache, dizziness, blurred vision and upset stomach are possible side effects [20] peptic ulcer disease, gastrointestinal bleeding and aspirin sensitivity are among conditions that make using NSAIDs contraindicated [21].

The enhanced solubility of esters and amides may improve bioavailability, hence reducing dose-dependent adverse effects [22-24]. In light of above observations, it is thought that ester derivatives of N-phenyl anthranilic acid compounds could be used to overcome the unwanted side effects of already existing fenamates. In present study, a series of ester derivatives of N-phenyl anthranilic acid are synthesized, characterized and the evaluated antimicrobial activities. Molecular docking studies using DNA gyrase (PDB ID: 4CKL) were also performed to better understand the mechanism of action of the synthesized molecules.

EXPERIMENTAL

Laboratory grade solvents and reagents were purchased from the different commercial suppliers. The TLC method was used to determine the R_f values of the synthesized derivatives. The capillary method melting point apparatus was used to determine the melting points of the synthesized ester derivatives and are uncorrected. The IR spectra were recorded on IR Spectrophotometer IR afiinity-1, Shimadzu using KBr Pallets. The ^{1}H NMR and ^{13}C NMR were obtained by using FT NMR Spectrometer Avance III, 400 MHz: Bruker by using solvents $CDCl_3$ and DMSO.

Synthesis of esters of N-phenyl anthranilic acid: An equimolar mixture of *N*-phenyl anthranilic acid and alkyl/aryl alcohols were placed in 250 mL round bottom flask fitted with an air condenser. A few drops of conc. H_2SO_4were added as a solvent and the mixture was boiled for 1 h. Cooled the solution mixture overnight and filtered the crude product. The precipitate obtained was recrystallized with diethyl ether and dried (**Scheme-I**).

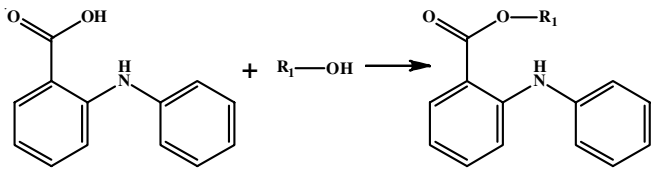

Scheme-I: Synthesis of ester derivatives of N-phenyl anthranilic acid (**MB 1-5**)

MB-1: 2-(Phenyl amino)methyl benzoate: Yield: 73%, m.p.: 170-172 ºC. R_f: 0.77 *m.f.*: $C_{14}H_{13}O_2N$ (*m.w.*: 227). IR (KBr, ν_{max}, cm^{-1}): 3043 (=C-H *str.* arom.), 1805 (-NH *str.*, br, 2º amine), 1660 (C=O *str.*, ester, br), 1581, 1512, 1440, 1410 (C=C *str.*, arom. ring), 1327 (C-H *bend.*, methyl) 1267, 1248 (-C-O *str.*, next to sp^2 carbon C=O), 1159 (CO-O-C *asym. str.*); ^{1}H NMR ($CDCl_3$, 400 MHz) δ ppm: 8.05-6.792 (multiplet, 9H, aromatic), 9.3 (broad singlet, 1H, NH), 3.5 (singlet, 3H, CH); ^{13}C NMR ($CDCl_3$, 400 MHz) δ ppm: 117 (C-1), 149 (C-2), 133 (C-3), 124.5 (C-4), 135.9 (C-5), 129.09 (C-6), 129.09 (C-8), 117 (C-9), 129.09 (C-10), 124 (C-11), 129.09 (C-12), 117 (C-13), 174 (C-14), 114.6 (C-16).

MB-2: 2-(Phenyl amino)ethyl benzoate: Yield: 72%, m.p.: 165-167 ºC. R_f: 0.77 *m.f.*: $C_{15}H_{15}O_2N$ (*m.w.*: 241). IR (KBr, ν_{max}, cm^{-1}): 3045 (=C-H *str.* arom.), 1811 (-NH *str.*, br, 2º amine), 1672 (C=O *str.*, ester, broad), 1591, 1500, 1440, 1421 (C=C *str.*, arom. ring), 1438, 1410 (C-H *bend.*, methylene), 1325 (C-H *bend.*, methyl), 1271, 1234 (-C-O *str.*, next to sp^2 carbon C=O), 1157 (CO-O-C *asym. str.*); ^{1}H NMR ($CDCl_3$, 400 MHz) δ ppm: 8.05-6.792 (multiplet, 9H, aromatic), 9.3 (broad singlet, 1H, NH), 4.4 (singlet, 2H, CH),1.3 (doublet, 3H, CH); ^{13}C NMR ($CDCl_3$, 400 MHz) δ ppm: 117 (C-1), 149 (C-2), 133 (C-3), 124.5 (C-4), 135.9 (C-5), 129.09 (C-6), 129.09 (C-8), 117 (C-9), 129.09 (C-10), 124 (C-11), 129.09 (C-12), 117 (C-13), 174 (C-14), 114.6 (C-16), 117 (C-17).

MB-3: 2-(Phenyl amino)isopropyl benzoate: Yield: 75%, m.p.: 176-178 ºC. R_f: 0.79 *m.f.*: $C_{16}H_{17}O_2N$ (*m.w.*: 255). IR (KBr, ν_{max}, cm^{-1}): 3041 (=C-H *str. arom.*), 2931, 2868 (C-H *str.*), 1813 (-NH *str.*, br, 2º-amine), 1660 (C=O *str.*), 1583, 1506, 1438 (C=C *str.*, arom. ring), 1325 (C-H *bend.*, methyl), 1267, 1248 (-C-O *str.*, next to sp^2 carbon C=O), 1159 (CO-O-C *asym. str.*); ^{1}H NMR ($CDCl_3$, 400 MHz) δ ppm: 8.05-6.792 (multiplet, 9H, arom.), 9.3 (broad singlet, 1H, NH), 4.1 (singlet, 1H, CH), 1.3 (broad singlet, 6H, CH); ^{13}C NMR ($CDCl_3$, 400 MHz) δ ppm: 117 (C-1), 147.08 (C-2), 133 (C-3), 124.5 (C-4), 135.9 (C-5), 129.09 (C-6), 129.09 (C-8), 117 (C-9), 129.09 (C-10), 124 (C-11), 129.09 (C-12), 117 (C-13), 174 (C-14), 114.6 (C-16), 117 (C-17), 117 (C-19).

MB-4: 2-(Phenyl amino)butyl benzoate: Yield: 68%, m.p.: 196-178 ºC. R_f: 0.23 *m.f.*: $C_{17}H_{19}O_2N$ (*m.w.*: 268). IR (KBr,

ν_{max}, cm^{-1}): 3045 (=C-H *str. arom.*), 1811 (-NH *str.*, br, 2º amine), 1670 (C=O stretching), 1587, 1496 (C=C *str.*, arom. ring), 1440, 1423 (C-H *bend.*, methylene), 1325 (C-H *bend.*, methyl), 1269, 1230 (-C-O *str.*, next to sp^2 carbon C=O), 1157 (CO-O-C *asym. str.*); ^{1}H NMR ($CDCl_3$, 400 MHz) δ ppm: 8.05-6.792 (multiplet, 9H, arom.), 9.3 (broad singlet, 1H, NH), 3.7 (singlet, 2H, CH), 1.6 (singlet, 2H, CH), 1.4 (singlet, 2H, CH), 0.9 (doublet, 3H, CH); ^{13}C NMR ($CDCl_3$, 400 MHz) δ ppm: 117 (C-1), 149 (C-2), 133 (C-3), 124.5 (C-4), 135.9 (C-5), 129.09 (C-6), 129.09 (C-8), 117 (C-9), 129.09 (C-10), 124 (C-11), 129.09 (C-12), 117 (C-13), 174 (C-14), 114.6 (C-16), 117 (C-17), 117 (C-18), 124 (C-19).

MB-5: 2-(Phenyl amino)phenyl benzoate: Yield: 63%, m.p.: 188-190 ºC. R_f: 0.41 *m.f.*: $C_{19}H_{15}O_2N$ (*m.w.*: 289). IR (KBr, ν_{max}, cm^{-1}): 3041 (=C-H *str. arom.*), 1811 (-NH *str.*, br, 2º amine), 1656 (C=O *str.*), 1577, 1508, 1440, 1421 (C=C *str.*, arom. ring), 1269, 1259, 1248 (-C-O *str.*, next to sp^2 carbon C=O), 1159 (CO-O-C *asym. str.*); ^{1}H NMR ($CDCl_3$, 400 MHz) δ ppm: 8.05-6.792 (multiplet, 9H, arom.), 9.3 (broad singlet, 1H, NH), 1.4 (multiplet, 5H, arom.); ^{13}C NMR ($CDCl_3$, 400 MHz) δ ppm: 149 (C-1), 124 (C-2), 114.6 (C-3), 117 (C-4), 114.6 (C-5), 124 (C-6), 174 (C-8), 114.06 (C-10), 117 (C-11), 129.09 (C-12), 135.9 (C-13), 124.5 (C-14), 133 (C-15), 124 (C-17), 117 (C-18), 129.09 (C-19), 124 (C-20), 129.09 (C-21), 120.9 (C-22).

Antibacterial activity: For antibacterial studies, ampicillin served as positive control and DMSO as negative control. Ampicillin and the text compounds were dissolved in DMSO to obtain 500 and 250 mM concentrations, respectively. The microorganism strains were seeded into samples of 15 mL nutritional agar media, which were then put into Petri plates. A wells of 8 mm were punched into the media and then filled with the test compounds. The plates were then incubated for 18 h at 37 ºC. The inhibitory zone's diameter (measured in mm) was used to evaluate the antibacterial activity. The average diameter of inhibitory zone was determined after each experiment was run in triplicate.

Docking: The crystal structure of DNA gyrase (PDB ID: 4CKL) was retrieved from the protein data bank (https://www.rcsb.org/) [25]. The crystal structure was prepared by removing existing ligands, water molecules, unbound ions and extra chains using PyMOL molecular graphics tool (Schrödinger, LLC). Thereafter, non-polar hydrogens were merged while polar hydrogens were added to the protein using Auto Dock tools and then saved into docking-ready PDBQT format [26]. The 2D chemical structures of all the ligands were drawn using Marvin Sketch 18.5.0 (Chem Axon Ltd.) and converted into 3D conformation (mol2 format). Polar hydrogens were added while non-polar hydrogens were merged with the carbon s and the internal degrees of freedom and torsions were set. The ligand molecules were further saved into the docking-ready PDBQT format using Auto Dock tools. Docking of the ligands to the target protein and determination of binding affinities was carried out using Auto Dock Vina [27].

Drug-likeness: *In silico* methods for determining the absorption, distribution, metabolism and excretion (ADME) parameters rely on statistically derived models generated by establishing relationships between the structural features of compounds and their biological responses [28]. Consequently, the ADME properties of the compound 73-KS5-51 were assessed using the SwissADME web tool [29] and Lipinski's rule of five was applied to evaluate its drug-likeness [30].

Toxicity: The test compounds were evaluated *in silico* for the prediction of possible toxicity of these compounds using the pkCSM online tool [31-33].

RESULTS AND DISCUSSION

A series of esters of N-phenyl anthranilic acid (**MB-1** to **MB-5**) were successfully synthesized as shown in **Scheme-I**. The purity of the prepared compounds was detected using silica gel-G TLC and was further elucidated by the spectral data.

The single peak observed at 3043 cm^{-1} in the FTIR spectrum of compound **MB-1** is attributed to =C-H stretching in the aromatic moiety. A broad signal was observed at 1805 cm^{-1} corresponding to –NH stretching in 2º amine. A peak at 1660 cm^{-1} indicates C=O stretching in an ester group, while a multiplet spectrum appeared at 1581, 1512, 1440 and 1410 cm^{-1}, corresponding to C=C stretching in aromatic rings. Additionally, the compound exhibited a peak at 1327 cm^{-1} due to C-H bending in a methyl group and double peaks were obser-ved at 1267 and 1248 cm^{-1} for C-O stretching adjacent to sp^2 carbon in C=O. A single peak at 1159 cm^{-1} for asymmetric stretching of CO-O-C. The ^{1}H NMR spectrum displays a multiplet signal ranging from δ 8.05 to 6.792 ppm for aromatic protons, along with a broad singlet observed at δ 9.3 ppm for the -NH proton. Additionally, a single signal at δ 3.5 ppm indicates the presence of methyl group protons. The ^{13}C NMR spectrum of the compound **MB-1** shows multiple peaks in the range of δ 149-124.5 ppm and 129.09-117 ppm corresponding to two benzene rings. A peak at δ 174 ppm corresponds to the carbonyl group of ester and another peak at δ 114.6 ppm corresponds to the methyl group of ester.

The appearance of a single peak at 3045 cm^{-1} in the FTIR spectrum of compound **MB-2** can be attributed to =C-H stretching in the aromatic moiety. A broad signal was observed at 1811 cm^{-1} corresponding to –NH stretching in 2º amine. A peak at 1672 cm^{-1} indicates C=O stretching in an ester group. Additionally, the peaks were observed at 1438 cm^{-1} and 1410 cm^{-1} for –CH bending of methylene group. The compound also exhibited a peak at 1325 cm^{-1} due to C-H bending in methyl group with double peaks observed at 1271 cm^{-1} and 1234 cm^{-1} for C-O stretching adjacent to sp^2 carbon in C=O. A single peak was observed at 1157 cm^{-1} for asymmetric stretching of CO-O-C. The ^{1}H NMR spectrum displays a multiplet signal ranging from δ 8.05 to 6.792 ppm for aromatic protons, along with a broad singlet observed at δ 9.3 ppm for the NH proton. Additionally, a single signal at δ 4.4 ppm corresponds to protons of methylene group and a doublet signal at δ 3.5 ppm indicates the presence of methyl group protons. The ^{13}C NMR spectrum of compound shows multiple peaks in the range of δ 149-117 ppm and δ 129.09-117 ppm corresponding to two benzene rings. A peak at δ 174 ppm corresponds to the carbonyl group of ester, while peaks at δ 114.6 ppm and 117 ppm correspond to the methylene group and methyl group of ester, respectively.

For compound **MB-3**, the FTIR spectrum shows a peak at 3041 cm^{-1}, which confirmed the =CH stretching in the aromatic

TABLE-1
ADME PROPERTIES OF THE N-PHENYL ANTHRANILIC ACID DERIVATIVES PREDICTED USING THE SWISS ADME WEB SERVER

Compound	MW	HBAs	HBDs	TPSA	MR	Log P	Log S	GI absorption
MB-1	227.26	2	1	38.33	67.27	2.59	-4.46 (Moderate)	High
MB-2	241.29	2	1	38.33	72.07	2.99	-4.68 (Moderate)	High
MB-3	255.31	2	1	38.33	76.88	2.75	-5.02 (Moderate)	High
MB-4	269.34	2	1	38.33	81.69	3.16	-5.23 (Moderate)	High
MB-5	289.33	2	1	38.33	87.39	2.54	-5.84 (Moderate)	High

MW: Molecular weight (g/mol); HBAs: Number of H-bond acceptors; HBDs: Number of H-bond donors; TPSA: Topological polar surface area (Å^2); MR: Molar refractivity; Log P: Partition coefficient; Log S: Estimated solubility (soluble, moderate or poor); GI absorption: Gastrointestinal absorption.

moiety. A broad signal observed at 1813 cm^{-1} corresponds to –NH stretching in a 2º amine. A peak at 1660 cm^{-1} indicates C=O stretching in an ester group, with additional peaks at 2931 cm^{-1} and 2868 cm^{-1} for C-H stretching. A multiplet peaks appeared at 1583 cm^{-1}, 1506 cm^{-1} and 1438 cm^{-1} correspond to C=C stretching in the aromatic rings. The compound also exhibited a peak at 1325 cm^{-1} due to C-H bending in methyl group, with double peaks observed at 1267 cm^{-1} and 1248 cm^{-1} for C-O stretching adjacent to sp^2 carbon in C=O. Another single peak at 1159 cm^{-1} was also observed for asymmetric stretching of CO-O-C. The ^{1}H NMR spectrum displays a multiplet signal ranging from δ 8.05 to 6.79 ppm for aromatic protons, along with a broad singlet observed at δ 9.3 ppm for the NH proton. Additionally, a single signal at δ 4.1 ppm corresponds to a CH proton whereas a single signal at δ 1.3 ppm indicates the presence of two methyl group protons. The ^{13}C NMR spectrum of compound **MB-3** shows multiple peaks in the range of δ 149-117 ppm and 129.09-117 ppm corresponding to two benzene rings. A peak at δ 174 ppm corresponds to the carbonyl group of the ester, while two peaks at δ 117 ppm and a peak at δ 114.6 ppm correspond to the presence of isopropyl group in ester. For compound **MB-4**, the FTIR spectrum shows a peak at 3045 cm^{-1} confirmed the =CH stretching in the aromatic moiety. A broad signal observed at 1811 cm^{-1} correspond to –NH stretching in 2º amine. A peak at 1670 cm^{-1} indicates C=O stretching in an ester group, with the additional peaks at 1440 cm^{-1} and 1423 cm^{-1} for C-H bending of the methylene group. The multiplet peaks appeared at 1587 cm^{-1} and 1496 cm^{-1} correspond to C=C stretching in aromatic rings. The compound also exhibited a peak at 1325 cm^{-1} due to C-H bending in a methyl group, with double peaks observed at 1269 cm^{-1} and 1230 cm^{-1} for C-O stretching adjacent to sp^2 carbon in C=O. The ^{1}H NMR spectrum displays a multiplet signal ranging from δ 8.05 to 6.79 ppm for aromatic protons, along with a broad singlet observed at δ 9.3 ppm for the -NH proton. Additionally, three singlet signals at δ 3.7, 1.6 and 1.4 ppm correspond to three CH_2 protons and a doublet signal at δ 0.9 ppm indicates the presence of CH_3 protons. The ^{13}C NMR spectrum shows the multiple peaks in the range of δ 149-117 ppm and 129.09-117.00 ppm correspond to two benzene rings. A peak at 174 ppm corresponds to the carbonyl group of ester, while the peaks at δ 114.6 ppm, 117 ppm and 124 ppm indicate the presence of butyl group.

The single peak observed at 3041 cm^{-1} in the FTIR spectrum of compound **MB-5** is attributed to =C-H stretching in the aromatic moiety. A broad signal was observed at 1811 cm^{-1} attributed to the –NH stretching in a secondary amine. A peak at 1660 cm^{-1} indicates C=O stretching in an ester group, while a multiplet spectrum appeared at 1577 cm^{-1}, 1508 cm^{-1}, 1440 cm^{-1} and 1421 cm^{-1}, corresponding to C=C stretching in aromatic rings. Additionally, the peaks were observed at 1269 cm^{-1}, 1259 cm^{-1} and 1248 cm^{-1} for C-O stretching adjacent to sp^2 carbon in C=O. The ^{1}H NMR spectrum displays a multiplet signal ranging from δ 8.05 to 6.79 ppm for aromatic protons, along with a broad singlet observed at δ ppm 9.3 for the NH proton. Additionally, a multiplet signal at δ 1.4 ppm corresponds to aromatic protons in the phenyl group. In ^{13}C NMR, the peak at δ 174 ppm corresponds to the carbonyl group of ester. Additionally, it displays three sets of peaks at 149-114.6 ppm, 114.6-135.9 ppm and 129.09-117 ppm, which correspond to three benzene rings, characteristic of a phenyl ester structure.

ADME study: The results obtained from the ADME study revealed that the synthesized compounds (**MB 1-5**) showed good pharmacokinetic parameters for oral bioavailability and drug-like properties (Table-1) as contrived by Lipinski's rule of five.

Antibacterial activity: Among the synthesized compounds, compound **MB-5** demonstrated significantly higher antibacterial activity against *E. coli* and *S. aureus* compared to other derivatives (Table-2). This enhanced activity is attributed to the presence of diphenyl group and its strategic position within the molecule.

TABLE-2
ANTIMICROBIAL ACTIVITY OF SYNTHESIZED N-PHENYL ANTHRANILIC ACID DERIVATIVES (**MB 1-5**)

Compd.	R^1	Zone of inhibition (mm)	
		Escherichia coli	*Staphylococcus aureus*
MB-1	CH_3	15 ± 0.5773	14 ± 0.5773
MB-2	CH_2CH_3	16 ± 1.0	15 ± 0.5773
MB-3	$CH(CH_3)_2$	22 ± 1.0	20 ± 1.154
MB-4	$(CH_2)_3CH_3$	18 ± 0.5773	18 ± 1.0
MB-5	C_6H_5	24 ± 0.5773	27 ± 1.154

Docking study: The docking protocol used in this study was first validated by redocking the respective co-crystallized ligand with DNA gyrase (PDB ID: 4CKL). The re-docked ligand of DNA gyrase produced pose similar to that of co-crystallized ligand DNA gyrase, indicating that a rational docking protocol used. The designed ester derivatives of N-phenyl anthranilic acid were docked with DNA gyrase (PDB entry: 4CKL) in order

to predict the binding interactions of these compounds with DNA gyrase. All the derivatives displayed appreciable bonding in the active site as determined by analyzing the hydrogen bonds, hydrophobic bonds and binding free energy (docking score, ΔG values, kcal/mol) of the chosen finest docked ligand-protein poses (Table-3).

The optimal docked conformation for compound **MB-5** was thoroughly analyzed using Discovery Studio to investigate its orientation, pattern, and binding interactions within the active site of DNA gyrase (Fig. 2). Compound **MB-5** showed the hydrogen bond interactions with Ser171 and Ser172 residues (with bond distance of 2.72 and 3.35 Å, respectively) and hydrophobic interactions with Lys45 & Arg91 residues (Pi-cation), His45 residue (Pi-Pi stacked) and Leu98 residue (Pi-alkyl). Docking of the newly synthesized of the N-phenyl anthranilic acid derivatives with the DNA gyrase protein revealed that these compounds bind potently with DNA gyrase and could serve as potential antibacterial agents inhibiting DNA gyrase.

Toxicity: The possible toxicity (mutagenic, carcinogenic, cardiotoxicity, immunotoxicity, skin irritation and reproductive toxicity) for the synthesized compounds (**MB 1-5**) was accessed using pkCSM online tool. Positive test results indicate that few compounds differs in terms of toxicity with each other (Table-4). For example, compounds **MB 3 and MB 5** are capable of producing hepatotoxicity. The LD_{50} was used as a reference standard for acute toxicity measurements.

Conclusion

The synthesis and characterization of ester derivatives of N-phenyl anthranilic acid (**MB 1-5**) with promising antibacterial activity demonstrated the potential for developing new antimicrobial agents. Compound **MB-5** [2-(phenyl amino)-phenyl

TABLE-3
DOCKING SCORE AND BINDING INTERACTIONS OF THE N-PHENYL ANTHRANILIC ACID DERIVATIVES WITH DNA GYRASE

Compd.	ΔG	Hydrogen bond interactions (bond distance)	Hydrophobic interactions (residues involved)
MB-1	-6.8	Gly170 (2.59 Å), Ser172 (2.97 Å) and Tyr266 (3.18 Å)	Pi-Pi Stacked (His45) and Pi-Alkyl (Leu98 & Tyr266)
MB-2	-6.4	Ser172 (3.07 Å)	Pi-Pi Stacked (His45) and Pi-Alkyl (Leu98)
MB-3	-6.5	Gly170 (2.54 Å) and Ser172 (3.10 Å)	Pi-Pi Stacked (His45) and Pi-Alkyl (His45 &Leu98)
MB-4	-5.9	Tyr266 (3.07 Å)	Pi-Cation (Lys45), Pi-Pi Stacked (His45), Alkyl (Arg91) and Pi-Alkyl (Leu98)
MB-5	-7.5	Ser171 (2.72 Å) and Ser172 (3.35 Å)	Pi-Cation (Lys45 & Arg91), Pi-Pi Stacked (His45) and Pi-Alkyl (Leu98)

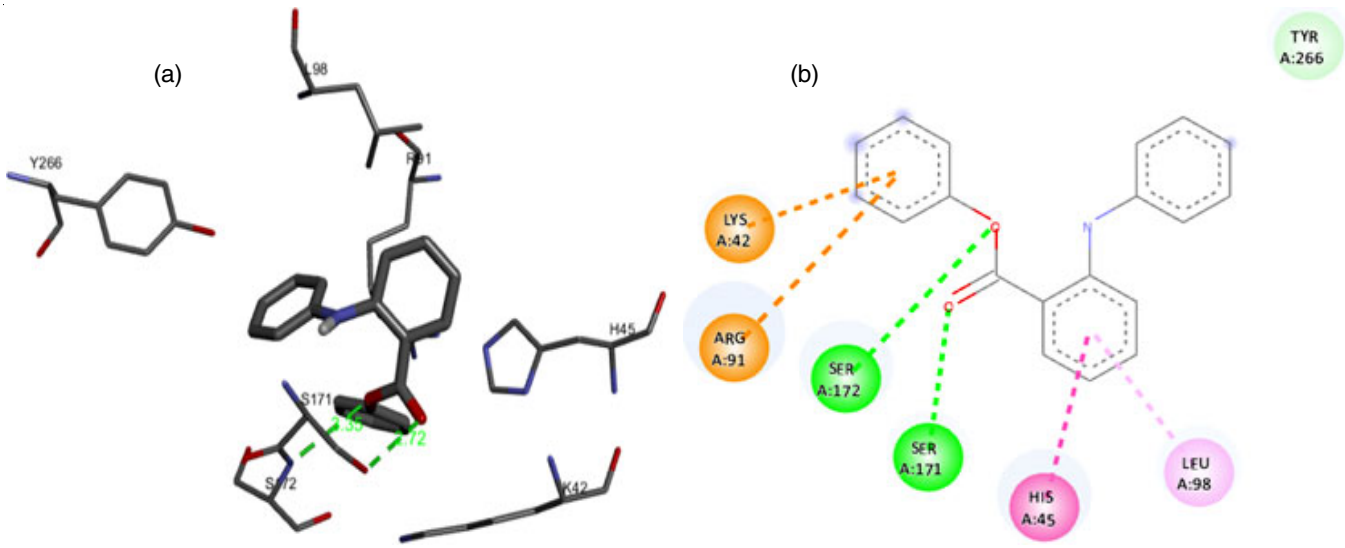

Fig. 2. Docking interaction analysis of **MB-5** with DNA gyrase. (a) 3D docked pose showing hydrogen bond interactions. (b) 2D docked pose showing hydrogen bond and hydrophobic interactions

TABLE-4
PROBABLE TOXICITY PREDICTION FOR THE DESIGNED COMPOUNDS OBTAINED USING THE pkCSM PROGRAM

Compd.	AMES toxicity	Max. tolerated dose (human)	hERG I inhibitor	hERG II inhibitor	Oral rat acute toxicity (LD_{50})	Oral rat chronic toxicity (LOAEL)	Hepato-toxicity	Skin Sensitization	*Tetrahymena pyriformis* toxicity	Minnow toxicity
MB-1	No	0.758	No	No	2.106	2.076	No	No	1.66	0.75
MB-2	No	0.812	No	No	2.157	2.098	No	No	1.71	0.58
MB-3	Yes	0.679	No	No	2.265	2.186	Yes	No	1.23	0.47
MB-4	Yes	0.951	No	Yes	2.189	2.251	No	No	1.52	0.41
MB-5	Yes	0.662	No	Yes	2.471	2.226	Yes	No	0.46	0.09

benzoate] exhibited highly antibacterial activities against *E. coli* and *S. aureus* than other compounds. The *in vitro* antimicrobial and *in silico* docking results showed a potential of these molecules to act as DNA gyrase inhibitors and these derivatives could serve as preliminary molecules for development of effective antimicrobial agents.

ACKNOWLEDGEMENTS

The authors are grateful to the authorities for the research facilities provided by Central Instrumentation Lab, Guru Jambheshwar University of Sciences and Technology, Hisar and Jan Nayak Ch. Devi Lal Memorial College of Pharmacy, Sirsa, India.

CONFLICT OF INTEREST

The authors declare that there is no conflict of interests regarding the publication of this article.

REFERENCES

1. P. Wiklund and J. Bergman, *Curr. Org. Synth.*, **3**, 379 (2006); https://doi.org/10.2174/157017906777934926
2. P. Prasher and M. Sharma, *Drug Dev. Res.*, **82**, 945 (2021); https://doi.org/10.1002/ddr.21842
3. T. Nasr, A. Aboshanab, K. Abouzid and W. Zaghary, *Egypt. J. Chem.*, **66**, 329 (2022); https://doi.org/10.21608/ejchem.2022.148409.6426
4. R.E. Williams, L. Cottrell, M. Jacobsen, L.R. Bandara, M.D. Kelly, S. Kennedy and E.A. Lock, *Biomarkers*, **8**, 472 (2003); https://doi.org/10.1080/13547500310001647030
5. H. Azuma, K. Banno and T. Yoshimura, *Br. J. Pharmacol.*, **58**, 483 (1976); https://doi.org/10.1111/j.1476-5381.1976.tb08614.x
6. I.-S. Kwon, J.H. Kwak, S. Pyo, H.-W. Lee, A. Kim and F.J. Schmitz, *J. Nat. Prod.*, **80**, 149 (2017); https://doi.org/10.1021/acs.jnatprod.6b00787
7. H. Schrey, F.J. Müller, P. Harz, Z. Rupcic, M. Stadler and P. Spiteller, *Phytochemistry*, **160**, 85 (2019); https://doi.org/10.1016/j.phytochem.2019.01.008
8. R. Teponno, S. Noumeur, S. Helaly, S. Hüttel, D. Harzallah and M. Stadler, *Molecules*, **22**, 1674 (2017); https://doi.org/10.3390/molecules22101674
9. F. Omar, N. Mahfouz and M. Rahman, *Eur. J. Med. Chem.*, **31**, 819 (1996); https://doi.org/10.1016/0223-5234(96)83976-6
10. H. Jiang, B. Zeng, G.-L. Chen, D. Bot, S. Eastmond, S.E. Elsenussi, S.L. Atkin, A.N. Boa and S.-Z. Xu, *Biochem. Pharmacol.*, **83**, 923 (2012); https://doi.org/10.1016/j.bcp.2012.01.014
11. M.C.P. Rees, R. Cañete-Solér, A. López Bernal and A.C. Turnbull, *Lancet*, **332**, 541 (1988); https://doi.org/10.1016/s0140-6736(88)92660-8.
12. M.K. Elgohary, M.S. Elkotamy, M.A. Alkabbani and H.A. Abdel-Aziz. *Bioorg. Chem.*, **147**, 107393 (2024); https://doi.org/10.1016/j.bioorg.2024.107393
13. A.P. Malykhina, F. Shoeb and H.I. Akbarali, *Eur. J. Pharmacol.*, **452**, 269 (2002); https://doi.org/10.1016/S0014-2999(02)02330-0
14. T. Suzuki, A. Hansen and M.C. Sanguinetti, *Biochim. Biophys. Acta Biomembr.*, **1858**, 783 (2016); https://doi.org/10.1016/j.bbamem.2015.12.024
15. P. Garg, *Biophys. J.*, **104**, 463A (2013); https://doi.org/10.1016/j.bpj.2012.11.2562
16. H. Hu, J. Tian, Y. Zhu, C. Wang, R. Xiao, J.M. Herz, J.D. Wood and M.X. Zhu, *Pflugers Arch.*, **459**, 579 (2010); https://doi.org/10.1007/s00424-009-0749-9
17. C. Klose, I. Straub, M. Riehle, F. Ranta, D. Krautwurst, S. Ullrich, W. Meyerhof and C. Harteneck, *Br. J. Pharmacol.*, **162**, 1757 (2011); https://doi.org/10.1111/j.1476-5381.2010.01186.x
18. J.-F. Sun, Y.-J. Xu, X.-H. Kong, Y. Su and Z.-Y. Wang, *Neurosci. Lett.*, **696**, 67 (2019); https://doi.org/10.1016/j.neulet.2018.12.008
19. K. Yamada, Y. Waniishi, R. Inoue and Y. Ito, *Japan. J. Pharmacol.*, **70**, 81 (1996); https://doi.org/10.1254/jjp.70.81
20. F. Buttgereit, G.R. Burmester and L.S. Simon, *Am. J. Med.*, **110**, 13 (2001); https://doi.org/10.1016/S0002-9343(00)00728-2
21. K.A. Metwally, S.H. Yaseen, E.-S.M. Lashine, H.M. El-Fayomi and M.E. El-Sadek, *Eur. J. Med. Chem.*, **42**, 152 (2007); https://doi.org/10.1016/j.ejmech.2006.09.001
22. S. Bala, S. Kamboj, V. Saini and D.N. Prasad, *J. Chem.*, **2013**, 412043 (2013); https://doi.org/10.1155/2013/412053
23. A. Husain, M.S.Y. Khan, S.M. Hasan and M.M. Alam, *Eur. J. Med. Chem.*, **40**, 1394 (2005); https://doi.org/10.1016/j.ejmech.2005.03.012
24. F.L. Lanza, *Am. J. Gastroenterol.*, **93**, 2037 (1998); https://doi.org/10.1111/j.1572-0241.1998.00588.x
25. M.P. Gleeson, A. Hersey and S. Hannongbua, *Curr. Top. Med. Chem.*, **11**, 358 (2011); https://doi.org/10.2174/156802611794480927
26. A. Daina, O. Michielin and V. Zoete, *Sci. Rep.*, **7**, 42717 (2017); https://doi.org/10.1038/srep42717
27. C.A. Lipinski, *Drug Discov. Today Technol.*, **1**, 337 (2004); https://doi.org/10.1016/j.ddtec.2004.11.007
28. H. Berman, K. Henrick and H. Nakamura, *Nat. Struct. Mol. Biol.*, **10**, 980 (2003); https://doi.org/10.1038/nsb1203-980
29. G.M. Morris, R. Huey, W. Lindstrom, M.F. Sanner, R.K. Belew, D.S. Goodsell and A.J. Olson, *J. Comput. Chem.*, **30**, 2785 (2009); https://doi.org/10.1002/jcc.21256
30. O. Trott and A.J. Olson, *J. Comput. Chem.*, **31**, 455 (2010); https://doi.org/10.1002/jcc.21334
31. D.E. Pires, T.L. Blundell and D.B. Ascher, *J. Med. Chem.*, **58**, 4066 (2015); https://doi.org/10.1021/acs.jmedchem.5b00104
32. A.C.F. Salgueiro, V. Folmer, H.S. da Rosa, M.T. Costa, A.A. Boligon, F.R. Paula, D.H. Roos and G.O. Puntel, *J. Ethnopharmacol.*, **194**, 6 (2016); https://doi.org/10.1016/j.jep.2016.08.048
33. D.E.V. Pires, L.M. Kaminskas and D.B. Ascher, *Methods Mol. Biol.*, **1762**, 271 (2018); https://doi.org/10.1007/978-1-4939-7756-7_14